
A FRAMEWORK FOR QUANTUM FINITE-STATE LANGUAGES WITH DENSITY MAPPING

SeungYeop Baik Sicheol Sung Yo-Sub Han

Yonsei University
Seoul, Republic of Korea
{sybaik2006,sicheol.sung,emmous}@yonsei.ac.kr

July 4, 2024

ABSTRACT

A quantum finite-state automaton (QFA) is a theoretical model designed to simulate the evolution of a quantum system with finite memory in response to sequential input strings. We define the language of a QFA as the set of strings that lead the QFA to an accepting state when processed from its initial state. QFAs exemplify how quantum computing can achieve greater efficiency compared to classical computing. While being one of the simplest quantum models, QFAs are still notably challenging to construct from scratch due to the preliminary knowledge of quantum mechanics required for superimposing unitary constraints on the automata. Furthermore, even when QFAs are correctly assembled, the limitations of a current quantum computer may cause fluctuations in the simulation results depending on how an assembled QFA is translated into a quantum circuit.

We present a framework that provides a simple and intuitive way to build QFAs and maximize the simulation accuracy. Our framework relies on two methods: First, it offers a predefined construction for foundational types of QFAs that recognize special languages MOD_n and EQU_k . They play a role of basic building blocks for more complex QFAs. In other words, one can obtain more complex QFAs from these foundational automata using standard language operations. Second, we improve the simulation accuracy by converting these QFAs into quantum circuits such that the resulting circuits perform well on noisy quantum computers.

Keywords Quantum finite-state automata · Quantum circuits · Framework · Closure properties · Error mitigation

1 Introduction

The scientific field of quantum mechanics inspired an advent of quantum computational models in the 1980s [1]. These models have enabled the development of quantum algorithms designed to tackle problems that are infeasible on classical computers, thus lending to their advantage. Investment in quantum computing has exploded with the recent development of physical quantum computers. With greater funding, research on quantum resource optimization has been explored across multiple fields, such as chemistry, quantum simulation and computational theory [2–5].

The intrinsic requirements of quantum algorithms propagate to the quantum computers on which they run. These requirements include the number of qubits, the accuracy of gates and topological structures. Currently, quantum computers fail to meet these requirements and rely on error suppression and error mitigation, both of which have implicit cost. Previous works have examined computational models with restrictions. [6–10]. We consider to use quantum finite-state automata (QFAs) that represent quantum computers with the restriction of limited qubits.

The concept of QFAs has been present since the inception of quantum computation [11], and extensive theoretical research has been conducted in this area [12–15]. However, the realization of QFAs as quantum circuits has only recently emerged with the introduction of functional quantum computers [16]. This research area is still in its early

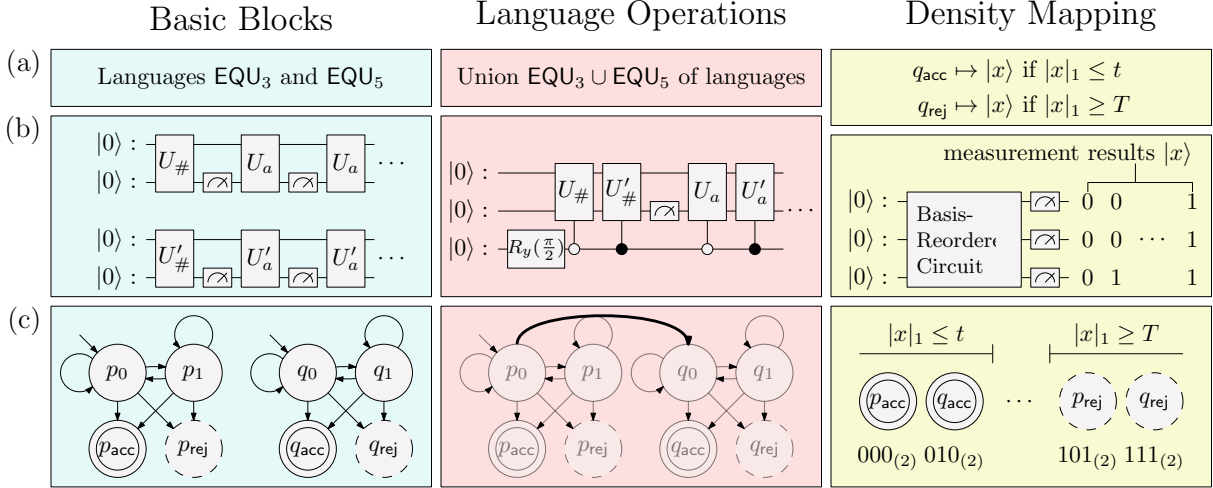


Figure 1: The three main features of our framework are as follows: basic blocks, language operations and density mapping. Each feature is presented in (a) a formal description, (b) a circuit and (c) a graphical representation.

stages, with researchers facing two main challenges: the difficulty of composing QFAs and the inaccuracies of quantum computers.

Constructing QFAs from scratch is challenging for those without knowledge of quantum mechanics or formal language theory. This complexity arises from the constraints on transitions in QFAs, where transitions must adhere to the properties of a unitary matrix. Properly constructed QFAs are still prone to obtaining practical results that deviate significantly from theoretical ones, due to the high error rate associated with quantum computers. This discrepancy is attributed to errors introduced during computation, which can alter the bit-representation of each state in the QFA circuit.

We propose a framework that addresses these challenges and enhances simulation accuracy by providing intuitive QFA composition methods alongside improvements to the transpilation process from QFAs to quantum circuits. Our framework enables users to compose complex QFAs from simple QFAs using language operations. Our proposed methodology extends the notable frameworks of classical automata, such as FAdo [17], FSA [18] and others [19–24]. In our proposed framework, we also introduce the novel concept of *density mapping*, a method employed in our framework for determining the bit-representation of each state in a QFA during transpilation. Density mapping is designed to reduce the probability of fluctuation caused by bit-flip errors. Fig. 1 demonstrates how a user can compose and simulate quantum circuits using the proposed framework. The intended workflow of our proposed framework is threefold: (1) constructing simple QFAs, (2) combining these simple QFAs with language operations to compose a *complex* QFA and (3) transpiling the resulting complex QFA into a circuit using density mapping. The given workflow lends to a more intuitive approach to quantum circuit construction as well as improved simulation accuracy therein.

In summary, we propose a framework that facilitates the construction and accurate simulation of QFAs. Our main contributions are as follows.

1. We introduce a novel QFA construction of unary finite languages, which serves as the elementary units of our framework.
2. We prove closure properties of various language classes defined by QFAs to illustrate how our framework combines QFAs.
3. We propose the \mathcal{D} -mapping technique to enhance the QFA simulation accuracy on quantum computers.

The rest of the paper is organized as follows. Section 2 provides a brief background on QFAs and their languages. In Section 3, we present details of our framework. We demonstrate the effectiveness of our density mapping in Section 4 by running experiments on the proposed framework. Finally, we summarize the results and outline possible future work in Section 5. Our framework is publicly accessible at <https://github.com/sybaik1/qfa-toolkit>.

2 Preliminaries

We first describe notations and definitions of two types of QFA: one is a measure-once (MO-) QFA and the other is a measure-many (MM-) QFA. We then define several types of languages recognized by MO-QFAs and MM-QFAs.

2.1 Basic Notations

Symbols \mathbb{R} and \mathbb{C} denote the set of real numbers and the set of complex numbers, respectively. For a finite set Q with n elements, \mathbb{C}^Q and $\mathbb{C}^{Q \times Q}$ denote the set of column vectors of dimensions n and the set of matrices of sizes (n, n) whose components are indexed by elements of Q and $Q \times Q$, respectively. For an element $a \in Q$, $|a\rangle \in \mathbb{C}^Q$ is a unit vector whose components are all zero, except an a -indexed component. The set $\{|a\rangle \mid a \in Q\}$ is a *standard basis* of the vector space $\mathbb{C}^{Q \times 1}$. A vector $\psi \in \mathbb{C}^{Q \times 1}$ has a unique expression as a linear combination:

$$\psi = \sum_{a \in Q} \alpha_a \cdot |a\rangle, \text{ where } \alpha_a \in \mathbb{C} \text{ for all } a \in Q.$$

Then, $|\psi| := \sqrt{\sum_{a \in Q} |\alpha_a|^2}$ denotes the *length* of ψ .

We use $\mathbf{M}^T, \mathbf{M}^{-1}, \overline{\mathbf{M}}$ and \mathbf{M}^\dagger to denote a *transpose, inverse, conjugate* and *conjugate-transpose* of a matrix \mathbf{M} , respectively. $\det \mathbf{M}$ denotes the *determinant* of a given matrix \mathbf{M} . A matrix \mathbf{U} is considered *unitary* if it satisfies the equality: $\mathbf{U}^{-1} = \mathbf{U}^\dagger$. Given a finite set A of indices and a set $S \subseteq A$, a projection matrix \mathbf{P}_S onto S is a zero-one diagonal matrix where $(\mathbf{P}_S)_{(a,a)} = 1$ if $a \in S$ and $(\mathbf{P}_S)_{(a,a)} = 0$, otherwise. For matrices $\mathbf{M}_1 \in \mathbb{C}^{A \times A}$ and $\mathbf{M}_2 \in \mathbb{C}^{B \times B}$ with $A \cap B = \emptyset$, their *direct sum* is

$$\mathbf{M}_1 \oplus \mathbf{M}_2 = \begin{bmatrix} \mathbf{M}_1 & \mathbf{0} \\ \mathbf{0} & \mathbf{M}_2 \end{bmatrix} \in \mathbb{C}^{(A \cup B) \times (A \cup B)}.$$

A *superposition* of n qubits is formalized as a 2^n -dimensional complex vector with a length of 1, and its evolution is described by a unitary matrix. The basis vectors of the superposition are represented by $|00 \cdots 0\rangle, |10 \cdots 0\rangle, \dots, |11 \cdots 1\rangle$, where each digit corresponds to the value of each qubit. The measurement of the superposition is formalized by an *observable*, which is a partitioning $A_1 \cup \cdots \cup A_k$ of the dimensions. When a superposition $|\psi\rangle$ is measured with an observable, it collapses to one of the vectors $|\psi'_i\rangle := P_{A_i} |\psi\rangle$, each with a probability $|\langle \psi'_i | \psi \rangle|^2$.

2.2 Quantum Finite-State Automata and Languages

A finite-state automaton (FA) is a model that simulates the behavior of a system changing its state between a fixed number of distinct states. The automaton updates its state in an online manner in response to external inputs—formalized as strings over a finite alphabet. A quantum finite-state automaton (QFA) is a quantum variant of FA, which can exist in a superposition comprised of a finite number of states. We consider two different types of QFAs: an MO-QFA, which is observed only at the end of sequential inputs [25], and an MM-QFA, which is observed after every step of the sequence [11].

Let Σ denote a finite *input alphabet*, which consists of the symbols used in sequential input. A *semi-QFA* then describes the evolution of a QFA for each symbol. Fig. 2 shows how transitions of a semi-QFA are represented graphically.

Definition 1. A *semi-QFA* is a tuple $(Q, \Sigma, \{\mathbf{U}_\gamma\}_{\gamma \in \Gamma})$, where (1) Q is a finite set of state, (2) $\{\mathbf{U}_\gamma\}_{\gamma \in \Gamma}$ is the unitary matrix for each symbol $\gamma \in \Gamma$ and (3) $\Gamma := \Sigma \cup \{\#, \$\}$ is the tape alphabet, with $\#$ and $\$$ as the start-of-string and end-of-string symbols, respectively.

We can define MO-QFAs and MM-QFAs as semi-QFAs with two defining distinctions: the inclusion of an initial state as well as that of final states, which are either accepting or rejecting.

Definition 2. An MO-QFA is specified by a tuple¹ $(Q, \Sigma, \{\mathbf{U}_\gamma\}_{\gamma \in \Gamma}, q_{init}, Q_{acc})$, where (1) a triple $(Q, \Sigma, \{\mathbf{U}_\gamma\}_{\gamma \in \Gamma})$ is a semi-QFA; (2) $q_{init} \in Q$ is an initial state; and (3) $Q_{acc} \subseteq Q$ is a set of accepting states.

An MO-QFA reads each symbol of string one by one and updates its superposition of states at each based on their transition matrix corresponding to the symbol. After reading the entire string, the MO-QFA measure the the superposition of states. It accepts the string if and only if the measured state is an accepting state; otherwise, it reject the string.

¹In some other papers, the tape alphabet of an MO-QFA does not include the end-of-string symbol. This does not affect the expressive power or the size of MO-QFAs [12].

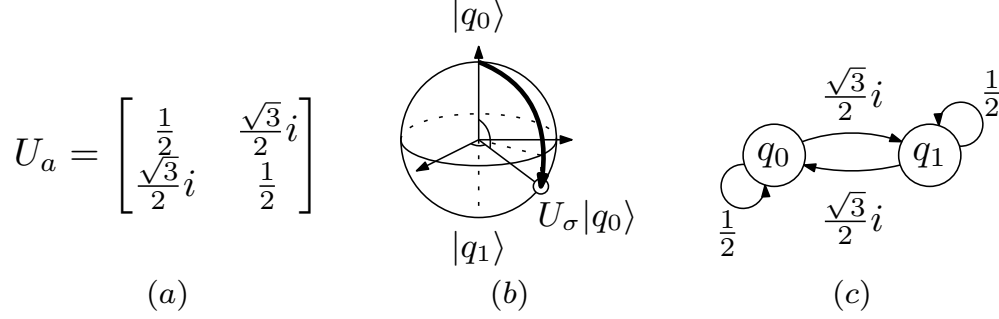


Figure 2: The relation between (a) a unitary transition matrix of a semi-QFA, (b) a change of superposition on the Bloch sphere according to a transition and (c) a graphical representation of the matrix's transitions. Transitions of QFAs, for example $|q_0\rangle \mapsto U_a |q_0\rangle$, are represented as a unitary transformation in Hilbert space.

Formally, for a string $x = x_1x_2 \cdots x_n \in \Gamma^*$ on the tape alphabet, we denote the unitary matrix $U_{x_n} U_{x_{n-1}} \cdots U_{x_1}$ as U_x . We also denote $\mathbf{P}_{Q_{\text{acc}}}$, $\mathbf{P}_{Q_{\text{rej}}}$ and $\mathbf{P}_{Q_{\text{non}}}$ as \mathbf{P}_{acc} , \mathbf{P}_{rej} and \mathbf{P}_{non} , respectively, for simplicity of notation. Then, the probability of an MO-QFA M accepting string w is $|\mathbf{P}_{\text{acc}} |\psi\rangle|^2$, where $|\psi\rangle$ is the superposition $U_{\#w\$} |q_{\text{init}}\rangle$ of the QFA after reading the end-of-string symbol.

Definition 3. An MM-QFA is specified by a tuple $(Q, \Sigma, \{\mathbf{U}_\gamma\}_{\gamma \in \Gamma}, q_{\text{init}}, Q_{\text{acc}}, Q_{\text{rej}})$, where (1) $(Q, \Sigma, \{\mathbf{U}_\gamma\}_{\gamma \in \Gamma})$ is a semi-QFA; (2) $q_{\text{init}} \in Q$ is an initial state; (3) $Q_{\text{acc}}, Q_{\text{rej}} \subseteq Q$ are sets of accepting and rejecting states, respectively. We denote a set of non-halting states $Q_{\text{non}} := Q \setminus (Q_{\text{acc}} \cup Q_{\text{rej}})$.

The MM-QFA reads the tape symbols one by one for a given string and updates the superposition according to the transition matrix, similar to MO-QFAs. However, unlike MO-QFAs, it measures their superposition at the end of each step, causing it to collapse onto one of three sub-spaces $\mathbb{C}^{Q_{\text{acc}}}$, $\mathbb{C}^{Q_{\text{rej}}}$ or $\mathbb{C}^{Q_{\text{non}}}$. The MM-QFA then accept or reject the string immediately if the resulting superposition is on $\mathbb{C}^{Q_{\text{acc}}}$ the MM-QFA M or $\mathbb{C}^{Q_{\text{rej}}}$, respectively. Otherwise, it keeps reading the next symbol.

Kondacs and Watrous [11] introduced *total states* to formalize the decision process of MM-QFAs. A total state is a triple $(\psi, p'_{\text{acc}}, p'_{\text{rej}}) \in \mathbb{C}^Q \times \mathbb{R} \times \mathbb{R}$, where p'_{acc} and p'_{rej} are the accumulated probabilities of acceptance and rejection. The vector ψ denotes the superposition and the probability of non-halting by its direction and the square of its length, respectively. For an MM-QFA M , T_γ is an evolution function of the internal state of M with respect to γ defined as follows:

$$T_\gamma : (\psi, p'_{\text{acc}}, p'_{\text{rej}}) \mapsto (\mathbf{P}_{\text{non}} \mathbf{U}_\gamma \psi, p'_{\text{acc}} + \Delta p'_{\text{acc}}, p'_{\text{rej}} + \Delta p'_{\text{rej}}),$$

where

$$\Delta p'_{\text{acc}} := |\mathbf{P}_{\text{acc}} \mathbf{U}_\gamma \psi|^2 \text{ and } \Delta p'_{\text{rej}} := |\mathbf{P}_{\text{rej}} \mathbf{U}_\gamma \psi|^2.$$

For a string $x = x_1x_2 \cdots x_n \in \Gamma^*$ on the tape alphabet, we use T_x to denote $T_{x_n} \circ T_{x_{n-1}} \circ \cdots \circ T_{x_1}$. Then, $(\psi, p_{\text{acc}}, p_{\text{rej}}) := T_{\#w\$}(|q_{\text{init}}\rangle, 0, 0)$ denotes the final total state, and p_{acc} is the probability that M accepts a given string w .

We say that an MM-QFA M is *valid* if $p_{\text{acc}} + p_{\text{rej}} = 1$ for any $w \in \Sigma^*$. If $p_{\text{acc}} = 0$ for every $w \in \Sigma^*$ such that $(_, p_{\text{acc}}, _) := T_{\#w\$}(|q_{\text{init}}\rangle, 0, 0)$, then we say that M is *end-decisive*. In other words, M does not accept strings before reading the end-of-string symbol. Similarly, M is *co-end-decisive* if it only rejects strings when reading the end-of-string symbol [12]. For the rest of the paper, we focus solely on valid MM-QFAs.

Let M be an MO-QFA or an MM-QFA and $f_M(w)$ denote the probability that a given M accepts w . We call the function $f_M : \Sigma^* \rightarrow \mathbb{R}$ the *stochastic language* of M . We say an MO- or MM-QFA M recognizes L with a *positive one-sided error* of margin $\varepsilon > 0$ if (1) $f_M(w) = 0$ for $w \notin L$ and (2) $f_M(w) > \varepsilon$. In other words, M always rejects $w \notin L$ and accepts $w \in L$ with probability $f_M(w) > \varepsilon$. Similarly, we say M recognizes L with a *negative one-sided error* of margin $\varepsilon > 0$ if (1) $f_M(w) = 1$ for $w \in L$ and (2) $f_M(w) < 1 - \varepsilon$ for $w \notin L$.

We define the following classes of *quantum finite-state languages (QFLs)* MOQFL, MMQFL, MMQFL_{end} and MMQFL_{coend} as those recognized by MO-QFAs, MM-QFAs, end-decisive MM-QFAs and co-end-decisive MM-QFAs, respectively. We also define the class of complements for each language family, which are denoted using a prefix co-. For example, co-MOQFL denotes the class $\{L \subseteq \Sigma^* \mid \bar{L} \in \text{MOQFL}\}$.

Table 1: The closure properties of stochastic languages f and g for each class of QFAs. Check mark (✓) and Cross mark (✗) denotes whether the class is closed under the operation or not.

QFA Class	$f_M \otimes f_N$	$c_1 f_M \oplus c_2 f_N$	$\overline{f_M}$	$h^{-1} \circ f_M$
MO-QFA	✓	✓	✓	✓
MM-QFA	✗	✓	✓	✓
End-dec.	✓	✓		✓
Co-end-dec.		✓		✓

2.3 Closure Properties of Stochastic Languages of QFAs

Stochastic languages of QFAs possess known closure properties, specific to MO-QFAs under the following operations [25, 13, 26].

(Hadamard product) $(f_M \otimes f_N)(w) = f_M(w) \cdot f_N(w)$

(Convex linear combination) For $c_1, c_2 \in [0, 1]$ with $c_1 + c_2 = 1$,

$$(c_1 f_M \oplus c_2 f_N)(w) = c_1 \cdot f_M(w) + c_2 \cdot f_N(w)$$

(Complement) $\overline{f_M}(w) = 1 - f_M(w)$

(Inverse homomorphism) $(h^{-1} \circ f_M)(w) = f_M(h^{-1}(w))$

Compared to the stochastic languages of MO-QFAs, those of MM-QFAs are closed under linear combination, complement and inverse homomorphism [13, 27] but not under the Hadamard product. For the cases of end-decisive and co-end-decisive MM-QFAs, their stochastic languages are closed under linear combination and inverse homomorphism. However, end-decisive MM-QFAs, in particular, are also closed under the Hadamard product [27]. Table 1 summarizes the closure properties of stochastic languages of QFAs. We also present a construction for the convex linear combination to complete the paper.

Proposition 1. *Consider two MM-QFAs*

1. $M := (Q, \Sigma, \{\mathbf{U}_\gamma\}_{\gamma \in \Gamma}, q_{init}, Q_{acc}, Q_{rej})$ and
2. $N := (P, \Sigma, \{\mathbf{V}_\gamma\}_{\gamma \in \Gamma}, p_{init}, P_{acc}, P_{rej})$.

For $c_1, c_2 \in [0, 1]$ with $c_1 + c_2 = 1$, the following MM-QFA $c_1 M \oplus c_2 N$ satisfies $(c_1 M \oplus c_2 N)(w) = c_1 M(w) + c_2 N(w)$.

$$c_1 M \oplus c_2 N := (Q \cup P, \Sigma, \{\mathbf{W}_\gamma\}_{\gamma \in \Gamma}, q_{init}, Q_{acc} \cup P_{acc}, Q_{rej} \cup P_{rej}),$$

where $\mathbf{W}_\gamma := \mathbf{U}_\gamma \oplus \mathbf{V}_\gamma$ for $\gamma \in \Sigma \cup \{\$\}$ and

$$\mathbf{W}_\# := (\mathbf{U}_\# \oplus \mathbf{V}_\#) \cdot \begin{bmatrix} \sqrt{c_1} & \mathbf{0} & i\sqrt{c_2} & \mathbf{0} \\ \mathbf{0} & \mathbf{I} & \mathbf{0} & \mathbf{0} \\ i\sqrt{c_2} & \mathbf{0} & \sqrt{c_1} & \mathbf{0} \\ \mathbf{0} & \mathbf{0} & \mathbf{0} & \mathbf{I} \end{bmatrix} \in \mathbb{C}^{(QU P) \times (QU P)}.$$

If M_1 and M_2 are both end-decisive or co-end-decisive, then the resulting M is also end-decisive or co-end-decisive, respectively.

3 Proposed Framework for QFLs

It is more complex to construct QFAs as opposed to classic FAs due to the unitary constraints that a QFA must preserve. On top of the difficulties with QFAs, when constructing a quantum circuit that recognizes a QFL, one has to consider a margin with the accepting probability and rejecting probability—the accepting policy [12, 28]. Several accepting policies exist, such as one-sided errors, two-sided errors, isolated cut-points, threshold acceptance and threshold with margin [13]. In our framework, we only consider one-sided errors since they offer a compromise between the language coverage and the closure properties.

When designing a quantum circuit for a language, a typical process of making their QFA proceeds as follows: First, determine the number of states for the target QFA. Then, construct transition matrices for each of the states adhering to

unitary constraints. Subsequently, verify if the created QFA can differentiate between accepting and rejecting strings. If it fails to do so, adjustments to the transitions design or an increase in the number of states are necessary. If the target QFA functions as intended, it can be transpiled into a quantum circuit.

The aforementioned process is not the sole paradigm of designing a circuit, but the continuous evolution of which, boasting both advancements and errors, are necessary in the development of the target quantum circuit. We overcome these errors and inconveniences by encapsulating the design process through the use of QFLs as building blocks. By doing so, we can employ operations between the building blocks to construct the desired QFL. In our framework, we provide constructions for the two languages MOD_p and EQU_k as building blocks, leveraging them to create more complex and diverse languages. In the above scenario, instead of deciding on the size and transitions, we can decompose the language into a set of expressions with MOD_p and EQU_k , then compose them to get the QFA. We can finally transpile the QFA with our density mapping to get the target quantum circuit.

3.1 Basic Blocks—Two QFLs with Simple Constructions

We settled on small and simple QFAs as the building blocks of our framework and give the characteristics and properties of two QFAs MOD_n and EQU_k .

First, we revisit $\text{MOD}_n := \{a^j \mid j \equiv 0 \pmod n\}$ that has several previous approaches due to its small and simple circuit [16]. It is known that there exists a two-state MO-QFA that recognizes the language MOD_n with a negative one-sided bounded error. Furthermore, for each prime p , there exists an $O(\log p)$ -state MO-QFA recognizing MOD_p with an error margin of $1/8$, which is independent of the choice of p . The circuit of MOD_n and MOD_p requires only one and $O(\log \log p)$ qubits, respectively [28]. Next, we present our construction of an MM-QFA for $\text{EQU}_k := \{a^k\}$.

Theorem 1. *Let $\{a\}$ be a unary alphabet. For a singleton language EQU_k , and parameters θ, φ with $0 < \theta, \varphi < \frac{\pi}{2}$, let $M_k(\theta, \varphi)$ be an co-end-decisive MM-QFA defined as follows.*

$$M_k := (Q, \{a\}, \{\mathbf{U}_\gamma\}_{\gamma \in \{\#, a, \$\}}, q_0, \{q_{\text{acc}}\}, \{q_{\text{rej}}\}),$$

where $Q := \{q_0, q_1, q_{\text{acc}}, q_{\text{rej}}\}$. The specific unitary operators are given by

$$\mathbf{U}_\# := \begin{bmatrix} \cos \theta & -\sin \theta & 0 & 0 \\ \sin \theta & \cos \theta & 0 & 0 \\ 0 & 0 & 1 & 0 \\ 0 & 0 & 0 & 1 \end{bmatrix}, \mathbf{U}_a := \begin{bmatrix} \cos \varphi & 0 & -\sin \varphi & 0 \\ 0 & 1 & 0 & 0 \\ \sin \varphi & 0 & \cos \varphi & 0 \\ 0 & 0 & 0 & 1 \end{bmatrix} \text{ and } \mathbf{U}_\$:= \sqrt{C_k} \cdot \begin{bmatrix} \mathbf{0} & \mathbf{A}_k^\dagger \\ \mathbf{A}_k & \mathbf{0} \end{bmatrix},$$

where \mathbf{A}_k is a sub-matrix given by

$$\mathbf{A}_k := \begin{bmatrix} \cos^k \varphi \cdot \cos \theta & \sin \theta \\ -\sin \theta & \cos^k \varphi \cdot \cos \theta \end{bmatrix},$$

and the factor C_k is given by $C_k := \cos^{2k} \varphi \cos^2 \theta + \sin^2 \theta$. Then, $M_k(\theta, \varphi)$ recognizes the language $\{a^k\}$ with a negative error bound with a margin ε satisfying

$$0 < \varepsilon < C_k^{-1} \cdot (\cos \theta \sin \theta \cos^k \varphi \cdot (1 - \cos \varphi))^2.$$

Proof. Fix $M := M_k(\theta, \varphi)$ for some parameters k, θ and φ . The validity of M is obvious from the construction. For each $j \geq 0$, let $T_{\#a^j}(|q_0\rangle, 0, 0) =: (\psi_j, p_{\text{acc},j}, p_{\text{rej},j})$. Then, the values of components are $\psi_0 = \mathbf{P}_{\text{non}} \mathbf{U}_\# |q_0\rangle = \cos \theta |q_0\rangle + \sin \theta |q_1\rangle$ and $\psi_{j+1} = \mathbf{P}_{\text{non}} \mathbf{U}_a \psi_j$. By induction, $\psi_j = \cos^k \varphi \cos \theta |q_0\rangle + \sin \theta |q_1\rangle$. Now we consider the final total state $T_{\#a^j \$}(|q_0\rangle, 0, 0) =: (\psi, p_{\text{acc}}(j), p_{\text{rej}}(j))$. The rejecting probability of a string a^j is

$$\begin{aligned} p_{\text{rej}}(j) &= |\mathbf{P}_{\text{rej}} \mathbf{U}_\$ \psi_j|^2 = |\mathbf{P}_{\text{rej}} \mathbf{U}_\$ (\cos^j \varphi \cos \theta \cdot |q_0\rangle + \sin \theta \cdot |q_1\rangle)|^2 \\ &= C_k^{-1} \cdot |(\cos^k \varphi - \cos^j \varphi) \cos \theta \sin \theta \cdot |q_{\text{rej}}\rangle|^2, \end{aligned}$$

and $M(a^k) = p_{\text{acc}}(k) = 1 - p_{\text{rej}}(k) = 1$. From the observation that $\arg \min_{j \neq k} p_{\text{rej}}(j) = k + 1$, we finally obtain

$$f_M(a^j) = 1 - p_{\text{rej}}(j) \leq 1 - p_{\text{rej}}(k + 1) = 1 - C_k^{-1} \cdot (\cos \theta \sin \theta \cos^k \varphi \cdot (1 - \cos \varphi))^2.$$

□

One might need to execute the QFA matching process multiple times to obtain a correct result, as the probability of obtaining the correct results decreases with the increasing length of the input string. The subsequent theorem describes how many repetitions are required to achieve a predetermined probability of accuracy.

Theorem 2. Fix the parameters θ_0, φ_0 and define $\alpha := \cos \theta_0$ and $\beta := \cos \varphi_0$. Let $M_k := M_k(\theta_0, \varphi_0)$ for each k . Then, $(M_k(a^j))^N < \frac{1}{e} \approx 0.37$ for each $j \neq k$, where

$$N := \frac{1}{(1 - \alpha^2)(1 - \beta)^2} + \frac{1}{\alpha^2 \beta^{2k}(1 - \beta)^2} - 1 \in 2^{\Omega(k)}.$$

Proof. Note that a^j has the minimum reject probability when $j = k + 1$, except in the case where $j = k$. We can compute the value of $M_k(a^{k+1})$ as follows:

$$\begin{aligned} M_k(a^{k+1}) &= 1 - \frac{(\cos \theta \cdot \sin \theta \cdot \cos^k \varphi (1 - \cos \varphi))^2}{\cos^{2k} \varphi \cdot \cos^2 \theta + \sin^2 \theta} \\ &= \frac{\alpha \beta^{2k} + (1 - \alpha^2) - \alpha^2 (1 - \alpha^2) \beta^{2k} (1 - \beta)^2}{\alpha^2 \beta^{2k} + (1 - \alpha^2)} \\ &= \left(1 + \frac{\alpha^2 (1 - \alpha^2) \beta^{2k} (1 - \beta)^2}{\alpha \beta^{2k} + (1 - \alpha^2) - \alpha^2 (1 - \alpha^2) \beta^{2k} (1 - \beta)^2} \right)^{-1} \\ &= \left(1 + \left(\frac{1}{(1 - \alpha^2)(1 - \beta)^2} + \frac{1}{\alpha^2 \beta^{2k}(1 - \beta)^2} - 1 \right)^{-1} \right)^{-1} \\ &= \left(1 + \frac{1}{N} \right)^{-1}. \end{aligned}$$

Then, $M_k(a^j)^N \leq M_k(a^{k+1})^N \leq (1 + \frac{1}{N})^{-N} < \frac{1}{e}$ for $j \neq k$. Therefore, when θ and φ are fixed independently of L_k , one have to run $M_k(\theta, \varphi)$ on w for $2^{\Omega(k)}$ -times to decide $w \in L_k$ within a fixed probability. \square

Note that Theorems 1 and 2 examine the condition where parameters θ and φ are chosen independently to the target language L_k . The following proposition describes how our framework finds optimal parameters that maximize the error margin for each k .

Proposition 2. Let ω be a unique positive solution of $\omega^{k+1} + (k + 1)\omega - k = 0$. Then, parameters $\theta = \tan^{-1} \sqrt{\omega^k}$ and $\varphi = \cos^{-1} \omega$ maximize the error margin of $M_k(\theta, \varphi)$.

Proof. We want to maximize the rejection probability $p_{\text{rej}}(\theta, \varphi)$ of a^{k+1} where

$$p_{\text{rej}}(\theta, \varphi) = \frac{(\cos \theta \sin \theta \cos^k \varphi (1 - \cos \varphi))^2}{\cos^{2k} \varphi \cos^2 \theta + \sin^2 \theta}.$$

Let $f(\theta, \varphi) := (p_{\text{rej}}(\theta, \varphi))^{-1}$ be an objective function. Then, the following holds.

$$\begin{aligned} (\theta_k, \varphi_k) &:= \arg \max_{\theta, \varphi} p_{\text{rej}}(\theta, \varphi) = \arg \min_{\theta, \varphi} f(\theta, \varphi) \\ &= \arg \min_{\theta, \varphi} \frac{1}{\sin^2 \theta (1 - \cos \varphi)^2} + \frac{1}{\cos^2 \theta \cos^{2k} \varphi (1 - \cos \varphi)^2} \end{aligned}$$

Since f is differentiable on the domain $0 < \theta, \varphi < \frac{\pi}{2}$, the equation $(\partial_{\theta} f)(\theta_k, \varphi_k) = (\partial_{\varphi} f)(\theta_k, \varphi_k) = 0$ holds. Then, we obtain the following equations from the partial derivatives of f with respect to θ and φ .

$$\begin{aligned} (\partial_{\theta} f)(\theta_k, \varphi_k) &= \frac{2 \sin \theta_k}{\cos^3 \theta_k \cos^{2k} \varphi_k (1 - \cos \varphi_k)^2} - \frac{2 \cos \theta_k}{\sin^3 \theta_k (1 - \cos \varphi_k)^2} \\ &= \frac{2 \tan^2 \theta_k \sin^2 \theta_k - 2 \cos^2 \theta_k \cos^{2k} \varphi_k}{\sin^2 \theta_k \cos^2 \theta_k \tan \theta_k \cos^{2k} \varphi_k (1 - \cos \varphi_k)^2} \\ &= \frac{2(\tan^2 \theta_k - \cos^k \varphi_k)(\tan^2 \theta_k + \cos^k \varphi_k)}{\sin^2 \theta_k \tan \theta_k \cos^{2k} \varphi_k (1 - \cos \varphi_k)^2} = 0 \end{aligned} \tag{1}$$

$$\begin{aligned} (\partial_{\varphi} f)(\theta_k, \varphi_k) &= \frac{2k \sin \varphi_k}{\cos^2 \theta_k \cos^{2k+1} \varphi_k (1 - \cos \varphi_k)^2} \\ &\quad - \frac{2 \sin \varphi_k}{(1 - \cos \varphi_k)^3} \left(\frac{1}{\sin^2 \theta_k} + \frac{1}{\cos^2 \theta_k \cos^{2k} \varphi_k} \right) = 0 \end{aligned} \tag{2}$$

Then, from Eq.s (1) and (2), we derive

$$\tan^2 \theta_k = \cos^k \varphi_k \quad (3)$$

and

$$k = \frac{\cos^{2k+1} \varphi_k \cos^2 \theta_k}{(1 - \cos \varphi_k)} \times \left(\frac{1}{\sin^2 \theta_k} + \frac{1}{\cos^{2k} \varphi_k \cos^2 \theta_k} \right),$$

respectively. Combining these equations, we obtain

$$\begin{aligned} k &= \frac{\cos^{2k+1} \varphi_k \cos^2 \theta_k}{(1 - \cos \varphi_k)} \times \left(\frac{1}{\sin^2 \theta_k} + \frac{1}{\cos^{2k} \varphi_k \cos^2 \theta_k} \right) \\ &= \frac{\cos \varphi_k \tan^4 \theta_k \cos^2 \theta_k}{(1 - \cos \varphi_k)} \times \left(\frac{1}{\sin^2 \theta_k} + \frac{1}{\tan^4 \theta_k \cos^2 \theta_k} \right) \quad (\because \text{Eq. (3)}) \\ &= \frac{\cos \varphi_k \sin^4 \theta_k}{(1 - \cos \varphi_k) \cos^2 \theta_k} \times \left(\frac{\sin^2 \theta_k + \cos^2 \theta_k}{\sin^4 \theta_k} \right) \\ &= \frac{\cos \varphi_k}{(1 - \cos \varphi_k)} \times \sec^2 \theta_k = \frac{\cos \varphi_k}{(1 - \cos \varphi_k)} \times (\tan^2 \theta_k + 1) \\ &= \frac{\cos \varphi_k}{(1 - \cos \varphi_k)} \times (\cos^k \varphi_k + 1) \quad (\because \text{Eq. (3)}) \\ &= \cos^{k+1} \varphi_k + (k + 1) \cos \varphi_k. \end{aligned}$$

Therefore, if ω is a unique positive solution of an equation $\omega^{k+1} + (k + 1)\omega - k = 0$, then the optimal parameters are $\theta_k = \tan^{-1} \sqrt{\omega^k}$ and $\varphi_k = \cos^{-1} \omega$. \square

3.2 Closure Properties of QFLs

In our framework, we consider Boolean operation over QFL, and distinguish the closure and error-bound properties of each operation. The closure operations are considered for each language class: MOQFL, MMQFL, MMQFL_{end} and MMQFL_{coend}. These also include the basic constructions of each language. Unlike other classes that are defined based on cut-points as mentioned in previous literature[12, 28], the properties of these classes have only been indirectly discussed. We examine properties of one-sided error-bounded languages, including closure properties for operations, to clarify how our framework supports the operations.

From an MO- and MM-QFA, we can obtain their complement QFAs by exchanging the set of accepting states and the set of rejecting states. We establish the following properties from the construction that transforms an end-decisive MM-QFA from a co-end-decisive MM-QFA and vice versa.

Property 1. *co-MOQFL and co-MMQFL are the class of languages recognized by MO-QFAs and MM-QFAs with a bounded positive one-sided error, respectively.*

The proof of Property 1 follows from the closure property of stochastic languages of QFAs under complement.

Proof. Let L be a co-MOQFL. By definition, \bar{L} is a MOQFL, meaning there exists an MO-QFA M and a margin $\epsilon > 0$ such that $w \in \bar{L} \equiv f_M(w) = 1$ and $w \notin \bar{L} \equiv f_M(w) < 1 - \epsilon$. Given that stochastic languages are closed under complement, we can construct another MO-QFA N such that $f_M(w) = 1 - f_N(w)$. Therefore, $w \notin L \equiv f_N(w) = 0$ and $w \in L \equiv f_N(w) > \epsilon$. Thus, MO-QFA N recognizes L with a bounded positive one-sided error. The proofs for the inverse direction are omitted for brevity. The proof for co-MMQFL is straightforward and follows similarly. \square

Property 2. *co-MMQFL_{end} and co-MMQFL_{coend} are the class of languages recognized by co-end-decisive and end-decisive MM-QFAs with a bounded positive one-sided error, respectively.*

Proof. Property 2 directly results from the way in which the complement of an MM-QFA is constructed, which involves swapping the end-decisiveness and co-end-decisiveness. In the proof of Property 1, if M is an end-decisive MM-QFA, then the corresponding MM-QFA N can be co-end-decisive, and vice versa. \square

We show that the operations are closed under stochastic language and correlate with the properties of QFLs.

Theorem 3. *Each class MOQFL, MMQFL, MMQFL_{end} and MMQFL_{coend} of languages is closed under intersection.*

Proof. The closure property of each language under intersection follows from the closure property of their corresponding QFAs under linear combination. \square

Theorem 4. *MOQFL and $\text{MMQFL}_{\text{coend}}$ are closed under union.*

Proof. Let L_1 and L_2 be languages in MOQFL. By Property 1, there exist MO-QFAs M_1 and M_2 recognizing $\overline{L_1}$ and $\overline{L_2}$ with a positive one-sided bounded error. Hence, there exists an MO-QFA M satisfying $f_M(w) = (f_{M_1} \otimes f_{M_2})(w)$ due to the closure property of MO-QFAs under Hadamard product. M recognizes $\overline{L_1} \cap \overline{L_2}$ with a positive one-sided error, and by Property 1 again, $\overline{L_1} \cap \overline{L_2} = L_1 \cup L_2$ is a MOQFL language. For the closure property of $\text{MMQFL}_{\text{coend}}$, we can utilize Property 2 instead of Property 1, and the closure property of end-decisive MM-QFAs with regard to the Hadamard product. \square

The next statement directly follows the fact that there exists a co-end-decisive MM-QFA for each unary finite language. The corollary leverages the closure property of $\text{MMQFL}_{\text{coend}}$ with regard to its union and the concept of singleton language construction from Theorem 1.

Corollary 1. *Every unary finite language is in $\text{MMQFL}_{\text{coend}}$.*

Table 2 summarizes the upper bounds of operational complexities as well as the complexities of inverse homomorphism and word quotient—both of which can be easily established from their constructions [25, 12].

Table 2: Upper bounds of operation complexities for QFL classes. Some of operations in this table are not yet supported by our framework. A dash (-) indicates that the upper bound of the operator is the same as the nearest non-empty row above.

QFL Class	Union	Intersection	Inverse Homo. (h^{-1})	Word Quotient ($w \setminus \cdot$)
MOQFL	nm	$n + m$	n	n
MMQFL		$n + m$	$n + c(h) \cdot n_{\text{halt}}$	$n + w \cdot n_{\text{halt}}$
MMQFL _{end}		$n + m$		
MMQFL _{coend}	nm	$n + m$		

$c(h)$ and n_{halt} denote the $\max |h(\sigma)|$ and $|Q_{\text{halt}}|$, respectively.

3.3 Density Mapping from QFA States to Qubit Basis Vectors

After a user composes QFAs for their QFLs using either simple constructions or language operations, the next step is to transpile these QFAs into quantum circuits. In the implementation of a QFA in a quantum computer with n qubits, each state of the QFA is represented with n -bits as one of 2^n basis vectors and the transitions are realized through a combination of quantum gates. Additionally, in the current era of noisy intermediate-scale quantum computing [29], we need to apply error mitigation methods that can compensate for possible errors.

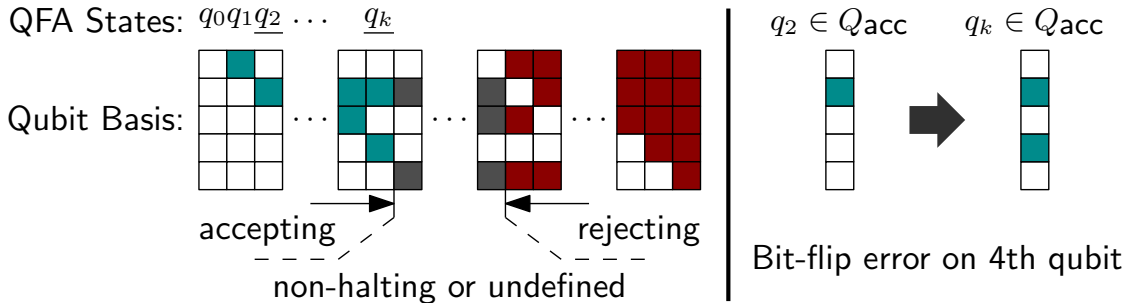


Figure 3: The expected error reduction of the proposed \mathcal{D} -mapping. The accepting state q_1 is mapped to the qubit basis $|10000\rangle$. If a bit-flip error occurs on the fourth qubit, then the measured qubit basis is $|10010\rangle$ that describes the state q_n . It does not effect whether or not the string is accepted because both q_1 and q_k are accepting.

We propose a technique called *density (\mathcal{D} -) mapping* which is applied before the transpilation stage of the quantum circuit. Rather than mapping QFA states to qubit basis vectors in an arbitrary manner, our \mathcal{D} -mapping reorders these

vectors based on the number of qubits with value 1. Then we assign the accepting and rejecting states to the basis vectors with a low and high number of qubits having the value 1, respectively.

\mathcal{D} -mapping maximizes the localization of accepting and rejecting states, thereby reducing the probability of bit-flip errors. These errors can arise from a decoherence or depolarization, and causes an accepting state to change into a rejecting state, and vice versa. Additionally, the basis vectors representing the accepting and rejecting states are separated by basis mapped to non-final states and basis that are not mapped to any states. This method helps to isolate the errors and reduce possible error situations. Fig. 3 conceptually illustrates how our proposal reduces a bit-flip error from altering the acceptance of a QFA.

4 Experimental Results and Analysis

We demonstrate the effectiveness of our \mathcal{D} -mapping with experiments using our framework. Our experiments measure how accurately quantum circuits simulate an operation of MOD_p of $O(\log p)$ states and EQU_k of 4 states by default construction. We compare the difference between ideal and experimental acceptance probabilities with and without the \mathcal{D} -mapping. We take 100,000 shots and measure the number of acceptances and rejections for each string.

We use IBM’s Falcon r5.11 quantum processor for real quantum experiments. When simulating the quantum circuits with controlled error rates, we utilize Qiskit simulators². The Qiskit simulator is configured to use the same basis gates and topological structure as the Falcon processor. We also set the error rates to follow the Falcon processor, except for the two types of errors—gate and readout errors. A mirroring factor η_g is applied to each error rate of gate G in the processor. The error rate of G in the simulator is calculated as follows:

$$(\text{Error rate of } G \text{ in the simulator}) = \eta_g \times (\text{Average error rate of } G \text{ in the processor}).$$

Readout errors are adjusted using the mirroring factor η_r and the readout error in the simulator is calculated similarly.

4.1 Difficulty of QFA simulation

We measured the MOD_5 language using the Falcon processor, as depicted in Fig. 4. This measurement was to demonstrate the current capabilities and state of quantum computers. Note that the automaton of MOD_5 accepts strings of length divisible by 5 with probability 1. Otherwise, it accepts the string with a probability less than 0.875. However, we can see that the measurements for the real-world computer accept strings with a probability close to 0.5. We analyze the low accuracy attributed to the large size of the resulting quantum circuit, exceeding 1,000 gates for even a length 2 input.

We also notice despite the small error rates of the simulator, the output of the simulator becomes inaccurate as the length of the string becomes longer. The inaccuracy is caused by the size of the circuit that grows linearly to the length of the input string. The accumulated errors eventually dominate and reduce the output closer to random guessing.

Our experiments from this point on are conducted using a quantum simulator to focus on the effectiveness of \mathcal{D} -mapping. We use error mirroring rates designed to reflect the capabilities of near-future quantum computers with error suppression and mitigation.

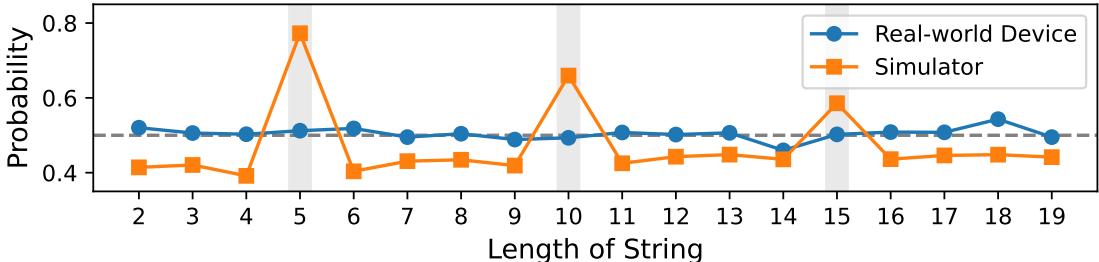


Figure 4: The experimental results for the language MOD_5 . Blue circles and orange squares indicate the accepting probability of strings, which are simulated on a real-world quantum computer and a simulator, respectively. The dashed line represents the 0.5 mark for random guessing. We set the mirroring factors η_g and η_r as 0.5%. In the case of an ideal computer with no errors, the accepting probabilities highlighted by gray boxes are 1.

²<https://www.ibm.com/quantum/qiskit>

4.2 Effectiveness of the Density Mapping on Simulators

We demonstrate the usefulness of our \mathcal{D} -mapping for emulating QFAs. We evaluate the accepting probability of input strings with the automaton of MOD_5 implemented by quantum circuits. Fig. 5 compares the experimental results for two quantum circuits recognizing MOD_5 , one utilizes our mapping and the other does not.

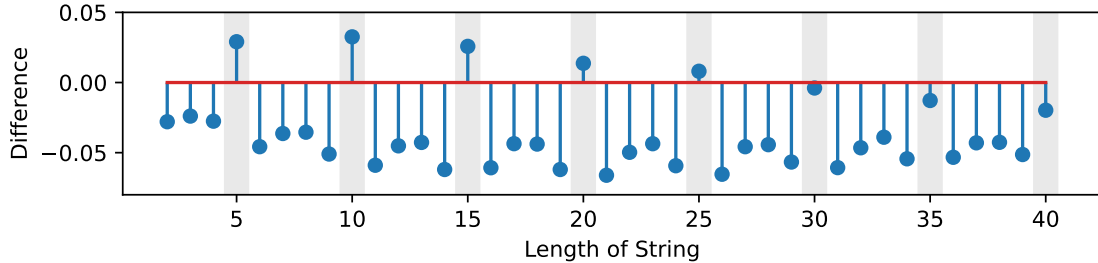


Figure 5: The difference in accepting probability from using the naive mapping to using \mathcal{D} -mapping on MOD_5 . We set the mirroring factors η_g and η_r as 0.5%. The blue dots above the red line represent the increase in accepting probability of \mathcal{D} -mapping compared to the naive mapping. Conversely, the blue dots below the red line represent the decrease in accepting probability. The strings highlighted with gray boxes should exhibit an increased accepting probability towards the ideal case, while other strings should show a decrease.

The experimental results confirm that \mathcal{D} -mapping increases the accuracy of the simulation for most cases. The mapping increases the accepting probability of strings in MOD_5 up to length 30 and decreases the accepting probability of strings that are not in MOD_5 . The effectiveness of \mathcal{D} -mapping diminishes with longer strings. Both mapping methods are increasingly affected by accumulating errors as discussed in Section 4.1, resulting in similar outcomes.

4.3 Effectiveness of the Density Mapping in Various QFAs

Table 3 presents the mean absolute percentage error (MAPE) of the experimental results for MOD_p and EQU_k implementations using the naive mapping and \mathcal{D} -mapping. Each cell denotes the dissimilarity between ideal probabilities $P(w_i)$ and measured $\bar{P}(w_i)$ for inputs w_1, \dots, w_n , and a simulation with a lower MAPE indicates higher accuracy. MAPE is calculated as follows:

$$\text{MAPE} = \frac{1}{n} \sum_{i=1}^k \left| \frac{P(w_i) - \bar{P}(w_i)}{P(w_i)} \right| \times 100(\%).$$

We use strings with length from 2 to 40 to compute the MAPE for each language. Note that the maximum achievable value of MAPE varies for each language, hence we cannot directly compare simulation accuracy between different languages using MAPE. For instance, consider the following cases: (1) $\eta_g = 0.1\%$ and $\eta_r = 0.1\%$; and (2) $\eta_g = 1\%$ and $\eta_r = 1\%$, where the latter case has greater error rate. Nevertheless, we use the according formulation to show the difference between probabilities and its difference.

The experimental results indicate that \mathcal{D} -mapping is effective for QFAs of languages MOD_3 , MOD_5 , but not for MOD_7 . \mathcal{D} -mapping reduces the difference between the accepting probabilities of ideal results and simulation for MOD_3 to 57.43%(1.43/2.49) of the former case and 46.24%(11.31/24.46) of the latter case. Similarly, for MOD_5 , \mathcal{D} -mapping reduces the difference to 80.49% and 59.97% of the former and latter case, respectively.

Note that the number of quantum circuit for MOD_p increases with the growth of p . We observe that the effect of \mathcal{D} -mapping is not evident for MOD_7 , as the simulation remains inaccurate regardless of the mapping used. This emphasizes the challenge posed by the large size of MOD_7 QFAs and the resulting quantum circuits, which involve a significant number of gates.

We also examine the impact of \mathcal{D} -mapping on QFAs of EQU_n , although its effect is less pronounced compared to MOD_p . Note that QFAs of EQU_n are MM-QFAs. Unlike MO-QFAs for MOD_p , simulations of MM-QFAs have the possibility of terminating before reading all symbols in each string. We suggest that the simulation for MM-QFAs receives less effect from gate errors because they may ignore trailing gates, thereby resulting in the reduced effectiveness of \mathcal{D} -mapping.

Table 3: The dissimilarity between the ideal results and the results of a simulator with naive and density mapping methods with mirroring factors (M.F.) η_g and η_r . Each value in the table represents the value of MAPE (%), which indicates the average dissimilarity in acceptance rates of strings.

M.F. (%)		Naive Mapping						Density Mapping					
η_g	η_r	MOD _p			EQU _n			MOD _p			EQU _n		
		$p = 3$	5	7	$n = 3$	5	7	3	5	7	3	5	7
0.1	0.1	2.49	1.64	1.35	0.07	0.08	0.07	1.43	1.32	1.35	0.06	0.07	0.07
	0.5	2.90	1.35	1.25	0.09	0.09	0.10	1.44	1.17	1.65	0.09	0.10	0.09
	1	2.82	1.85	1.43	0.10	0.11	0.08	1.92	1.21	1.66	0.13	0.11	0.10
0.5	0.1	12.76	7.44	5.80	0.10	0.09	0.11	6.13	4.85	6.22	0.11	0.11	0.11
	0.5	13.08	7.16	6.01	0.14	0.17	0.13	6.24	4.64	6.04	0.14	0.13	0.16
	1	12.86	7.10	5.87	0.19	0.17	0.20	6.08	4.85	6.25	0.18	0.15	0.18
1	0.1	24.18	13.83	11.02	0.19	0.21	0.18	11.66	8.39	10.94	0.19	0.19	0.19
	0.5	24.26	13.73	10.91	0.23	0.20	0.23	11.37	8.28	11.21	0.22	0.18	0.22
	1	24.46	13.94	11.18	0.25	0.23	0.29	11.31	8.36	11.15	0.24	0.26	0.27

The overall experimental results reveal that gate error rates dominate simulation accuracy for QFAs, and our experiments do not show a clear relation between readout error rates and simulation accuracy. This is primarily due to the fact that the quantum circuits for QFAs have few measurement gates.

5 Conclusions and Future Work

MO-QFA and MM-QFA are the two most simplest quantum computational models. Despite their simple structure, designing these models is complex because their transitions must satisfy the unitary constraints. Verification is also challenging due to the low accuracy of current quantum devices. We have developed the framework to facilitate easy construction and accurate simulation of QFAs. For the development of the framework, we have

- composed a novel construction for EQU_k,
- demonstrated the closure properties of MOQFL, MMQFL, MMQFL_{end} and MMQFL_{coend},
- introduced \mathcal{D} -mapping to improve the accuracy of experiments on real-world devices,
- showcased the basic functionalities of our framework.

Our experiments on real devices highlight a significant limitation of current quantum processors—the QFA simulations on these processors are close to the random guessing due to their low accuracy. On the other hand, the experimental results confirm that our density mapping increases the accuracy of the QFA simulations.

A major limitation of our framework is its inability to construct QFAs from a human-readable format while most FA frameworks support a direct FA construction from regular expressions. Furthermore, manual construction remains inevitable for some languages because some types of QFLs cannot be obtained by composing MOD_p and EQU_k. We aim to characterize the class of languages by identifying which languages and operations can generate these classes. We will then integrate these languages and operations into our framework and enable users to construct a broader variety of languages more easily.

Our density mapping technique reduces simulation errors by correlating each QFA state with an appropriate dimension of a quantum circuit. The accuracy in quantum circuits can also be increased by reducing the number of gates [16] or by assigning more physical qubits to represent a single logical qubit [30]. The interaction between the density mapping and these existing methods may affect their overall effectiveness. Thus, it is another future work to integrate our density mapping with other techniques for improving the overall performance.

References

- [1] Paul Benioff. The computer as a physical system: A microscopic quantum mechanical hamiltonian model of computers as represented by Turing machines. *Journal of statistical physics*, 22:563–591, 1980. doi: <https://doi.org/10.1007/BF01011339>.

- [2] Mahzabeen Emu, Salimur Choudhury, and Kai Salomaa. Quantum neural networks driven stochastic resource optimization for metaverse data marketplace. In *2023 IEEE 9th International Conference on Network Softwarization (NetSoft)*, pages 242–246, 2023. doi: <https://doi.org/10.1109/NetSoft57336.2023.10175433>.
- [3] Juan Miguel Arrazola, Alain Delgado, Bhaskar Roy Bardhan, and Seth Lloyd. Quantum-inspired algorithms in practice. *Quantum*, 4:307, 2020. doi: [10.22331/q-2020-08-13-307](https://doi.org/10.22331/q-2020-08-13-307).
- [4] Matthew Hagan and Nathan Wiebe. Composite quantum simulations. *Quantum*, 7:1181, 2023. doi: [10.22331/q-2023-11-14-1181](https://doi.org/10.22331/q-2023-11-14-1181).
- [5] Robbie King. An improved approximation algorithm for quantum max-cut on triangle-free graphs. *Quantum*, 7:1180, 2023. doi: [10.22331/q-2023-11-09-1180](https://doi.org/10.22331/q-2023-11-09-1180).
- [6] Harumichi Nishimura and Masanao Ozawa. Perfect computational equivalence between quantum Turing machines and finitely generated uniform quantum circuit families. *Quantum Information Processing*, 8:13–24, 2009. doi: <https://doi.org/10.22331/q-2023-03-20-956>.
- [7] Harumichi Nishimura. Quantum computation with restricted amplitudes. *International Journal of Foundations of Computer Science*, 14(05):853–870, 2003. doi: <https://doi.org/10.1142/S0129054103002059>.
- [8] Aida Gainutdinova and Abuzer Yakaryılmaz. Unary probabilistic and quantum automata on promise problems. *Quantum Information Processing*, 17:1–17, 2018. doi: <https://doi.org/10.1007/s11128-017-1799-0>.
- [9] Lucas B Vieira and Costantino Budroni. Temporal correlations in the simplest measurement sequences. *Quantum*, 6:623, 2022. doi: <https://doi.org/10.22331/q-2022-01-18-623>.
- [10] Ruo Cheng Huang, Paul M Riechers, Mile Gu, and Varun Narasimhachar. Engines for predictive work extraction from memoryful quantum stochastic processes. *Quantum*, 7:1203, 2023. doi: <https://doi.org/10.22331/q-2023-12-11-1203>.
- [11] Attila Kondacs and John Watrous. On the power of quantum finite state automata. In *38th Annual Symposium on Foundations of Computer Science, FOCS '97, Miami Beach, Florida, USA, October 19-22, 1997*, pages 66–75, 1997. doi: <https://doi.org/10.1109/SFCS.1997.646094>.
- [12] Alex Brodsky and Nicholas Pippenger. Characterizations of 1-way quantum finite automata. *SIAM Journal on Computing*, 31(5):1456–1478, 2002. doi: <https://doi.org/10.1137/S0097539799353443>.
- [13] Alberto Bertoni, Carlo Mereghetti, and Beatrice Palano. Quantum computing: 1-way quantum automata. In *Developments in Language Theory, 7th International Conference, DLT 2003, Szeged, Hungary, July 7-11, 2003, Proceedings*, volume 2710, pages 1–20, 2003. doi: https://doi.org/10.1007/3-540-45007-6_1.
- [14] Andris Ambainis, Ashwin Nayak, Amnon Ta-Shma, and Umesh Vazirani. Dense quantum coding and a lower bound for 1-way quantum automata. In *Proceedings of the thirty-first annual ACM symposium on Theory of computing*, pages 376–383, 1999. doi: <https://doi.org/10.1145/301250.301347>.
- [15] Konstantinos Giannakis, Christos Papalitsas, and Theodore Andronikos. Quantum automata for infinite periodic words. In *2015 6th International Conference on information, intelligence, systems and applications (IISA)*, pages 1–6. IEEE, 2015. doi: <https://doi.org/10.1109/IISA.2015.7388105>.
- [16] Utku Birkan, Özlem Salehi, Viktor Olejár, Cem Nurlu, and Abuzer Yakaryılmaz. Implementing quantum finite automata algorithms on noisy devices. In *Computational Science - ICCS 2021 - 21st International Conference, Krakow, Poland, June 16-18, 2021, Proceedings, Part VI*, volume 12747, pages 3–16, 2021. doi: https://doi.org/10.1007/978-3-030-77980-1_1.
- [17] André Almeida, Marco Almeida, José Alves, Nelma Moreira, and Rogério Reis. FAdo and GUItar. In *Implementation and Application of Automata, 14th International Conference, CIAA 2009, Sydney, Australia, July 14-17, 2009. Proceedings*, volume 5642, pages 65–74, 2009. doi: https://doi.org/10.1007/978-3-642-02979-0_10.
- [18] Stephan Kanthak and Hermann Ney. FSA: An efficient and flexible C++ toolkit for finite state automata using on-demand computation. In *Proceedings of the 42nd Annual Meeting of the Association for Computational Linguistics (ACL-04)*, pages 510–517, 2004. doi: <https://doi.org/10.3115/1218955.1219020>.
- [19] Hamoon Mousavi. Automatic theorem proving in Walnut. *arXiv*, abs/1603.06017, 2016. doi: <https://doi.org/10.48550/arXiv.1603.06017>.
- [20] Mehryar Mohri, Fernando C. N. Pereira, and Michael Riley. A rational design for a weighted finite-state transducer library. In *Automata Implementation, Second International Workshop on Implementing Automata, WIA '97, London, Ontario, Canada, September 18-20, 1997, Revised Papers*, volume 1436 of *Lecture Notes in Computer Science*, pages 144–158. Springer, 1997. doi: <https://doi.org/10.1007/BFb0031388>.

- [21] Cyril Allauzen, Michael Riley, Johan Schalkwyk, Wojciech Skut, and Mehryar Mohri. OpenFst: A general and efficient weighted finite-state transducer library. In Jan Holub and Jan Zdárek, editors, *Implementation and Application of Automata, 12th International Conference, CIAA 2007, Prague, Czech Republic, July 16-18, 2007, Revised Selected Papers*, volume 4783, pages 11–23, 2007. doi: https://doi.org/10.1007/978-3-540-76336-9_3.
- [22] Jonathan May and Kevin Knight. Tiburon: A weighted tree automata toolkit. In *Implementation and Application of Automata, 11th International Conference, CIAA 2006, Taipei, Taiwan, August 21-23, 2006, Proceedings*, volume 4094, pages 102–113, 2006. doi: <https://doi.org/10.1007/978-3-031-07469-1>.
- [23] Denis Arrivault, Dominique Benielli, François Denis, and Rémi Eyraud. Scikit-SpLearn: a toolbox for the spectral learning of weighted automata compatible with scikit-learn. In *Conference francophone sur l'Apprentissage Automatique*, 2017. URL <https://hal.science/hal-01777169/>.
- [24] Walter S. Brainerd. Tree generating regular systems. *Information and Control*, 14(2):217–231, 1969. doi: [https://doi.org/10.1016/s0019-9958\(69\)90065-5](https://doi.org/10.1016/s0019-9958(69)90065-5).
- [25] Cristopher Moore and James P. Crutchfield. Quantum automata and quantum grammars. *Theoretical Computer Science*, 237(1-2):275–306, 2000. doi: [https://doi.org/10.1016/S0304-3975\(98\)00191-1](https://doi.org/10.1016/S0304-3975(98)00191-1).
- [26] Andris Ambainis, Arnolds Kikusts, and Māris Valdatš. On the class of languages recognizable by 1-way quantum finite automata. In *Annual Symposium on Theoretical Aspects of Computer Science*, pages 75–86, 2001. doi: https://doi.org/10.1007/3-540-44693-1_7.
- [27] Maria Paola Bianchi and Beatrice Palano. Behaviours of unary quantum automata. *Fundamenta Informaticae*, 104(1-2):1–15, 2010. doi: <https://doi.org/10.3233/FI-2010-333>.
- [28] Andris Ambainis and Rusins Freivalds. 1-way quantum finite automata: Strengths, weaknesses and generalizations. In *39th Annual Symposium on Foundations of Computer Science, FOCS '98, November 8-11, 1998, Palo Alto, California, USA*, pages 332–341, 1998. doi: <https://doi.org/10.1109/SFCS.1998.743469>.
- [29] John Preskill. Quantum computing in the NISQ era and beyond. *Quantum*, 2:79, 2018. doi: <https://doi.org/10.22331/q-2018-08-06-79>.
- [30] Joydip Ghosh, Austin G Fowler, and Michael R Geller. Surface code with decoherence: An analysis of three superconducting architectures. *Physical Review A*, 86(6):062318, 2012. doi: <https://doi.org/10.1103/PhysRevA.86.062318>.